Likewise, in Tie2Δcyto–GFP-expressing CHO cells, Tie2Δcyto–GFP was found at cell–substratum contacts, indicating the requirement of the extracellular domain of Tie2 for this localization. These Tie2–GFP positive structures at cell–substratum contacts were located close to, but apparently different from, vinculin-marked FCs or focal adhesions (FAs) (Supplementary Information, Fig. S4c). To identify the cell matrix junctions where Tie2 localizes, we carefully compared Tie2–GFP with those of various markers for FCs and FAs in HUVECs plated on fibronectin- and collagen-coated dishes after COMP–Ang1 stimulation. Tie2–GFP at cell–substratum contacts colocalized with none of these markers including vinculin, paxillin, VASP, and talin (Supplementary Information, Fig. S5a–g). Collectively, these results indicate that upon stimulation with Ang1, Tie2 is recruited to the cell periphery and anchored to substratum contacts that are different from FCs and FAs. This is further supported by time-lapse imaging using HUVECs expressing Tie2–GFP and CHO cells expressing either Tie2–GFP or Tie2Δcyto–GFP upon COMP–Ang1 stimulation (Supplementary Information, Movie 6 and 7).

$\alpha_5\beta_1$ integrin associates with fibronectin fibrils to form distinct adhesive structures from FCs and FAs, namely fibrillar adhesions (FBs) where fibrinogenesis occurs[24,25]. Since Cascone *et al.* has reported that Tie2 constitutively associates with $\alpha_5\beta_1$ integrin that binds to fibronectin[26], we examined whether Tie2 localizes at FBs. When Tie2–GFP– or HA-tagged Tie2 (Tie2–HA)–expressing HUVECs plated on a fibronectin-coated dish were stimulated with COMP–Ang1, Tie2 did not colocalize with FB markers (α_5 integrin, assembled fibronectin fibrils and exogenously expressed GFP–tensin) (Supplementary Information, Fig. S5h–j). In addition, depletion of α_5 integrin by siRNA did not affect COMP–Ang1-induced Tie2 localization at cell–substratum contacts (Supplementary Information, Fig. S6a–d). Depletion of another integrin, $\alpha_v\beta_3$, did not alter COMP–Ang1-induced relocation of Tie2 to peripheral cell–substratum contacts (Supplementary Information, Fig. S6 a–c).

We assumed that Ang1 might anchor Tie2 to extracellular matrix (ECM). When Tie2–GFP-expressing CHO cells were sparsely cultured on collagen-coated dishes and stimulated with COMP–Ang1, Tie2–GFP and FLAG-tagged COMP–Ang1 were clearly colocalized at the periphery and bottom of the cells at 5 min after stimulation, with the appearace of a ring (Fig. 3c). After 30 min, we noticed that Ang1 was detected not only with Tie2–GFP but also on the dish surface where the cell was not present (Fig. 3c and Supplementary Information, Fig. S6e), suggesting that Ang1 can bind to ECM. Indeed, Ang1 and COMP–Ang1, but not control protein, could bind to fibronectin, collagen, and vitronectin with high affinity, and bind weakly to laminin and fibrinogen as demonstrated by an ECM–Ang1 binding assay (Fig. 3d and Supplementary Information, Fig. S6f). Adhesive structures formed at cell–substratum contacts such as FCs and FAs are resistant to detergent (0.5% Triton-X100)[27,28]. Whereas Tie2–GFP but not RFP–Crk disappeared upon detergent addition without pretreatment of COMP–Ang1, pretreatment of COMP–Ang1 preserved Tie2–GFP at the bottom of cells as well as RFP–Crk and vinculin (Fig. 3e). These results suggest that Tie2 is anchored by ECM-bound Ang1 to cell–substratum contacts to form novel detergent-resistant adhesive structures, which are different from FCs, FAs and FBs.

Preferential activation of Erk and Akt in the absence and presence of cell–cell contacts upon Ang1 stimulation

We investigated the biological significance of *trans*-associated Tie2 at cell–cell contacts and cell–substratum contact-anchored Tie2 upon Ang1 stimulation. Tie2 under both conditions was phosphorylated at either cell–cell contacts or cell–substratum contacts (Fig. 4a). The extent of Tie2 phosphorylation in HUVECs by COMP–Ang1 did not depend upon the presence of cell–cell contacts (Fig. 4b, c).

Among Tie2-mediated signalling factors[4,19], Akt and Erk are suggested to be important for cell survival, and cell migration and proliferation, respectively[9,29,16,30,31]. We therefore checked the requirement of Tie2 in Ang1-induced Erk and Akt activation in HUVECs, because Ang1 is known to mediate some biological functions through integrins [32,33]. Ang1-dependent phosphorylation of both Erk and Akt in confluent and sparse HUVECs was abolished by depletion of Tie2 (Fig. 4d and data not shown). Under either sparse or confluent culture conditions, COMP–Ang1 induced Erk phosphorylation, which peaked at 10 min after stimulation and declined to the basal level by 45 min (Fig. 4e). However, the maximum level of Erk phosphorylation in the confluent cells was reduced to approximately 50% of that in the sparse cells (Fig. 4e). In clear contrast, the maximum increase in Akt phosphorylation was significantly higher in the confluent cells than in the sparse cells (Fig. 4e), indicating that endothelial cell–cell adhesions positively regulate the Tie2-mediated Akt pathway. We noticed that this preferential activation of Akt was a Tie2-specific signal in the confluent cell culture, because both Erk and Akt activation was suppressed when the endothelial cells were stimulated with growth media in the presence of cell–cell contacts (Fig. 4f).

Activation of Erk by Tie2 at cell–substratum contacts is partly dependent upon focal adhesion kinase and involved in endothelial cell migration

To further explore how Tie2-mediated signalling in isolated cells is influenced by its targeting to cell–substratum contacts, HUVECs were stimulated with COMP–Ang1 under either suspended or substratum-attached conditions. While Tie2 phosphorylation and subsequent Akt activation were comparable between these conditions, Erk activation was higher in substratum-attached cells (Fig. 5a). Similar results were obtained using BaF3 cells stably expressing Tie2 (BaF–Tie2) (Supplementary Information, Fig. S7a–c). These findings suggest that Erk activation by Ang1–Tie2 requires the contacts between cells and substratum, as previously reported for other receptor tyrosine kinases[34,35].

We hypothesized that Ang1–Tie2 at cell–substratum contacts cooperatively function with integrin signalling complexes to induce Erk activation, although Tie2 localized to cell–substratum contacts besides FCs, FAs and FBs. To test this possibility, we examined whether ECM-anchored Ang1 induces Tie2 signalling and modulates integrin adhesions. In HUVECs adhering to a collagen-coated dish, Tie2 diffusely localized at bottom surface of the cells. In clear contrast, Tie2 was found to be punctate and phosphorylated at cell–substratum contacts when the cells were attached to a collagen- and COMP–Ang1-coated dish (Supplementary Information, Fig. S7d, e), indicating the capability of ECM-anchored Ang1 to stimulate Tie2. HUVECs adhering to collagen- and COMP–Ang1-coated substratum exhibited enhanced vinculin accumulation at the most peripheral region of the cells, compared with the cells attached to collagen, as analysed by line-scanning of immunofluorescence intensity (Fig. 5b, c). Consistently, fewer stress fibres and more lamellipodia were observed in the presence of COMP–Ang1 (Supplementary Information, Fig. S7f). These data reveal that Ang1–Tie2 signalling at cell–substratum contacts induces FC formation.

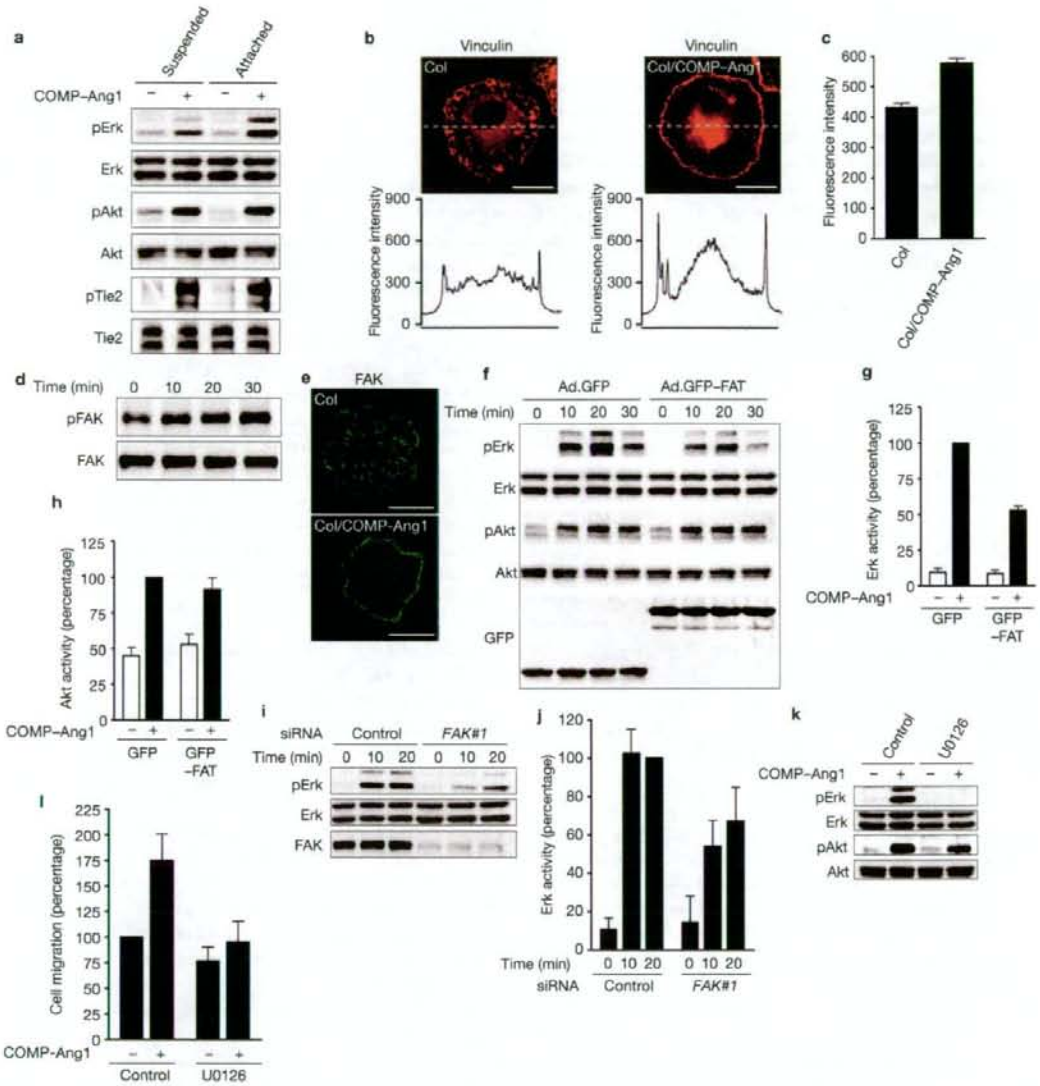

Figure 5 Activation of Erk by Tie2 at cell–substratum contacts partly depends upon FAK and is involved in endothelial cell migration. (**a**) Suspended HUVECs and cells adhered on a as described in Supplementary Methods. (**b**) HUVECs were placed on the COMP–Ang1–unbound collagen-coated dish (Col) or COMP–Ang1–bound collagen-coated dish (Col and COMP–Ang1) for 30 min, and immunostained with anti-vinculin antibody. Focal complexes were analysed by line intensity scan using MetaMorph 6.1 software (fluorescence intensity along the dotted line indicated, bottom panels). (**c**) Quantification of the Results of **b**. Values are expressed as means ± s.d. of fluorescence intensity relative to vinculin at the cell periphery (Col, $n = 60$; Col & COMP–Ang1, $n = 66$). (**d**) Sparse HUVECs starved for 6 h were stimulated with COMP–Ang1 for different times (min). Immunoprecipitates and cell lysate were subjected to western blot analysis with anti-phosphotyrosine (pFAK) and anti-FAK (FAK) antibodies, respectively. (**e**) Localization of FAK was examined similarly to **b**. (**f**) Sparse HUVECs plated on a collagen-coated dish were infected with adenovirus vector encoding either GFP or GFP–FAT as described in Supplementary Information, Methods. Cells stimulated with COMP–Ang1 for 20 min were analysed for Erk and Akt activation. (**g**, **h**) Phosphorylation of Erk (g) and Akt (**h**) in **f** was quantified. Values are expressed as means ± s.d. from five independent experiments. (**i**) Effect of knockdown of FAK on Erk activation was examined in control siRNA (control) or *FAK* siRNA-treated HUVECs (FAK No.1). (**j**) Quantification of the results of **i**. Values are expressed as means ± s.d. from 6 independent experiments. (**k**, **l**) MEK–Erk inhibition results in decreased migration of sparse HUVECs stimulated with COMP–Ang1. 20 μM U0126 (a MEK inhibitor) inhibits COMP–Ang1-induced Erk, but not Akt activation (**k**). Migration of HUVECs was analysed as described in Supplementary Methods (**l**). Values are expressed as the mean ± s.d. from 5 independent experiments. The scale bars represent 20 μm (**b**, **e**). Uncropped images of **a**, **d**, **f**, **i**, **k** are shown in Supplementary Information, Fig. S8.

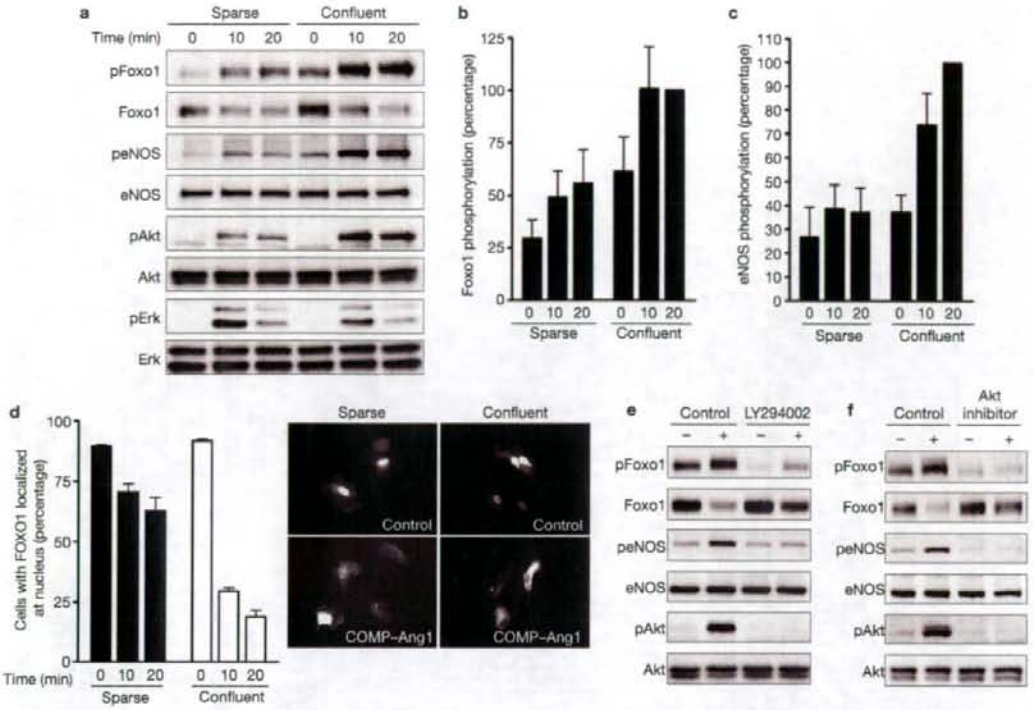

Figure 6 The presence of cell–cell contacts determines the preferential activation of Akt and subsequent phosphorylation of Foxo1 and eNOS. (**a**) Sparse and confluent HUVECs were starved and stimulated with COMP–Ang1. Cell lysates were analysed for phosphorylation of Foxo1, eNOS, Akt, and Erk. Note that Foxo1 and eNOS are more phosphorylated in the confluent cells than in the sparse cells. (**b**) COMP–Ang1–induced phosphorylation of Foxo1 observed in **a** was quantified. Foxo1 phosphorylation represents the ratio of phosphorylated Foxo1 to total Erk protein as a percentage of the ratio in the confluent cells stimulated for 20 min. Erk protein but not Foxo1 was used as normalization for protein loading, because anti-Foxo1 antibody does not recognize phosphorylated Foxo1. Values are expressed as means ± s.d. from seven independent experiments. (**c**) COMP–Ang1-induced phosphorylation of eNOS observed in **a** was quantified. eNOS phosphorylation represents the ratio of phosphorylated eNOS to total eNOS as a percentage of the ratio in the confluent cells stimulated for 20 min. Values are expressed as means ± s.d. from seven independent experiments. (**d**) Sparse and confluent HUVECs transfected with a plasmid encoding GFP–Foxo1 were starved for 6 h and stimulated with COMP–Ang1 for the time (min) as indicated. After fixation in methanol, the number of cells with GFP–Foxo1 localized at nucleus was counted and expressed as a percentage relative to total number of cells. At least 100 GFP-positive cells were scored for each treatment. Values are expressed as means ± s.d. from three independent experiments. Representative images of subcellular localization of GFP–Foxo1 in sparse (left) and confluent (right) cells are shown on the bottom. Upper and lower panels show the images in cells stimulated with vehicle or COMP–Ang1 for 20 min. (**e**, **f**) Confluent HUVECs were pre-treated with 20 μM LY294002 for 30 min (**e**) or 8 μM Akt inhibitor for 5 min (**f**) and subsequently stimulated with vehicle (–) or COMP–Ang1 (+) for 20 min. The effect of both inhibitors on COMP–Ang1-induced phosphorylation of Foxo1, eNOS, and Akt was examined. Uncropped images of **a**, **e**, and **f** are shown in Supplementary Information, Fig. S8.

Focal adhesion kinase (FAK) localizing at FCs and FAs mediates signalling by integrins and growth factor receptors to activate Erk[36,37]. Previously, it has been reported that Ang1 activates FAK to induce endothelial cell sprouting[13]. Thus, we tested the involvement of FAK in Erk activation downstream of cell–substratum contact-anchored Tie2 upon Ang1 stimulation. COMP–Ang1 induced tyrosine phosphorylation and accumulation of FAK to FCs in HUVECs (Fig. 5d and Supplementary Information, Fig. S7g) and increased the FAK-positive FC assembly as well as vinculin (Fig 5b, e). Consistent with the idea that the focal-adhesion-targeting domain of FAK (FAT) displaces FAK from FCs and FAs[36], overexpression of RFP-tagged FAT (RFP–FAT) perturbed the localization of FAK to FCs and FAs in HUVECs (Supplementary Information, Fig. S7h). Tie2 localization at peripheral cell–substratum contacts upon COMP–Ang1 stimulation was not influenced by overexpression of FAT (Supplementary Information, Fig. S7i). We next investigated the effect of FAT on Tie2-mediated intracellular signalling. Overexpression of GFP-tagged FAT (GFP–FAT) significantly but not completely inhibited COMP–Ang1-induced Erk activation (Fig. 5f, g). In clear contrast, overexpression of FAT did not alter COMP–Ang1-induced Akt activation (Fig. 5f, h). Furthermore, depletion of FAK by siRNAs partly inhibited COMP–Ang1-induced Erk activation (Fig. 5i, j and Supplementary Information, Fig. S7j, k). Collectively, these results indicate that Erk activation by Tie2 anchored to cell–substratum contacts is ascribed partly to FAK.

Erk signalling is known to be involved in endothelial cell migration[38]. Thus, we examined the role of Erk in cell migration by Ang1–Tie2 at cell–substratum contacts. Cell motility was enhanced when HUVECs

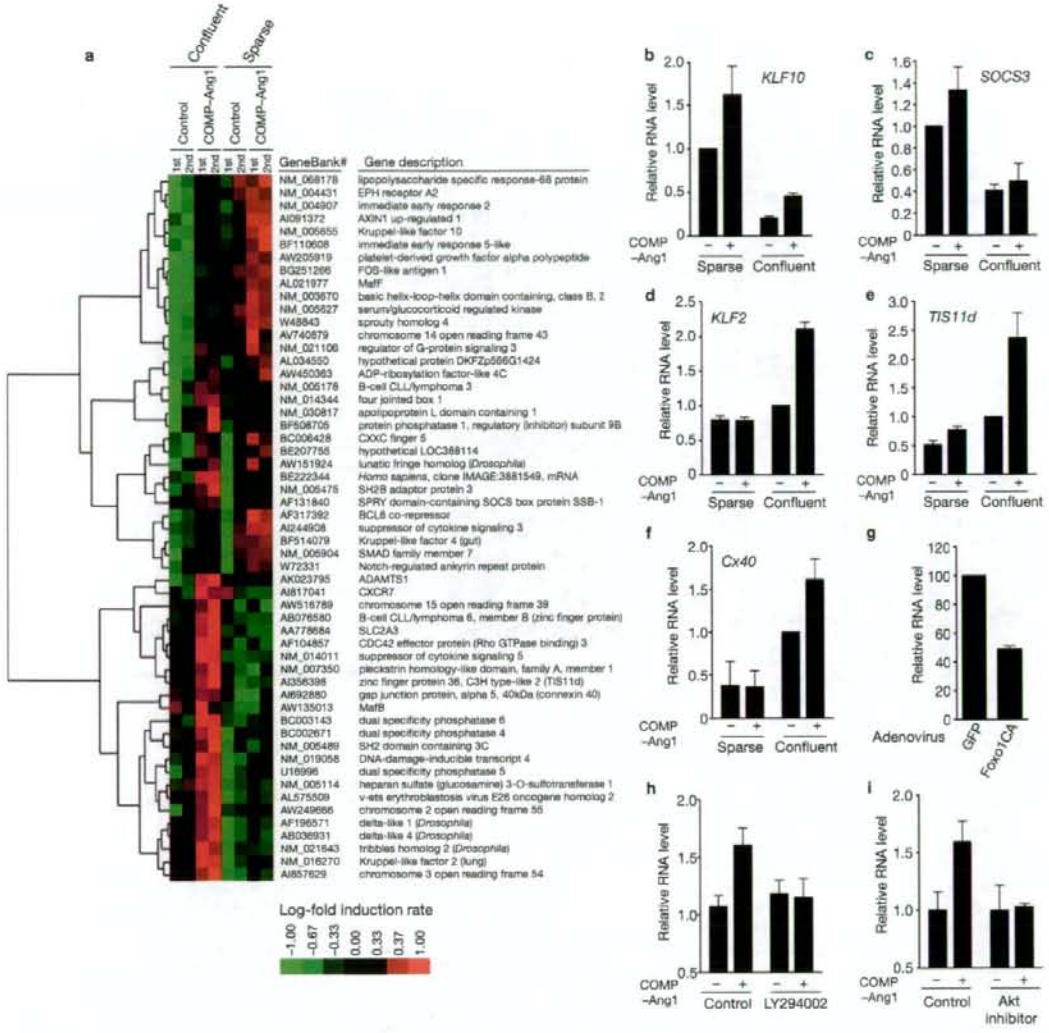

Figure 7 Ang1 stimulation leads to a distinct pattern of gene expression in HUVECs in the presence or absence of cell–cell contacts. (**a**) Total RNA was purified from confluent and sparse HUVECs stimulated with vehicle (control) or COMP–Ang1 for 1 h, and subjected to Affymetrix microarray analysis, as described in Methods. Genes corresponding to the criteria described in Methods were subjected to the cluster analysis. The results from two independent microarray analyses are displayed. Red and green represent higher and lower expression than the median for that particular gene, respectively. Color intensity is related to the difference with the median (black). (**b**–**f**) Total RNA was purified from confluent and sparse HUVECs stimulated with vehicle (–) or COMP–Ang1 (+) for 1 h, and expression levels of *KLF10* (**b**), *SOCS3* (**c**), *KLF2* (**d**), *TIS11d* (**e**) and *Cx40* (**f**) were analysed by real-time RT–PCR analysis as described in Supplementary Information, Methods. Bar graphs show relative RNA levels of each gene normalized to GAPDH levels. RNA levels are expressed relative to that in sparse (**b**, **c**) or confluent (**d**–**f**) cells stimulated with vehicle. Values are expressed as means ± s.d. from more than three independent experiments. (**g**) Total RNA was isolated from confluent HUVECs infected with adenovirus vectors encoding either GFP (GFP) or a constitutively active mutant of Foxo1 (Foxo1CA). Expression levels of *Cx40* were analysed as described for **f**, and expressed as a percentage relative to that in cells infected with GFP-encoding adenovirus vector. (**h**) Confluent HUVECs were stimulated with COMP–Ang1 in the presence (LY294002) or absence (control) of LY294002 as described in the legend of Fig. 6e. Expression levels of *Cx40* were analysed as described for **f**. Data are means ± s.d. of triplicate samples, and similar results were obtained in three independent experiments. (**i**) Confluent HUVECs were stimulated with COMP–Ang1 in the presence (Akt inhibitor) or absence (control) of Akt inhibitor as described in the legend of Fig. 6f. Expression levels of *Cx40* were analysed and expressed as described for **h**.

were placed on collagen- and COMP–Ang1-coated transwell filters, compared with cells adhering to collagen-coated filters. This enhanced cell motility was cancelled by inhibiting Erk using U0126, a MEK inhibitor (Fig. 5k, l). These findings suggest that Ang1–Tie2 at cell–substratum contacts regulates endothelial cell migration through the Erk signalling pathway.

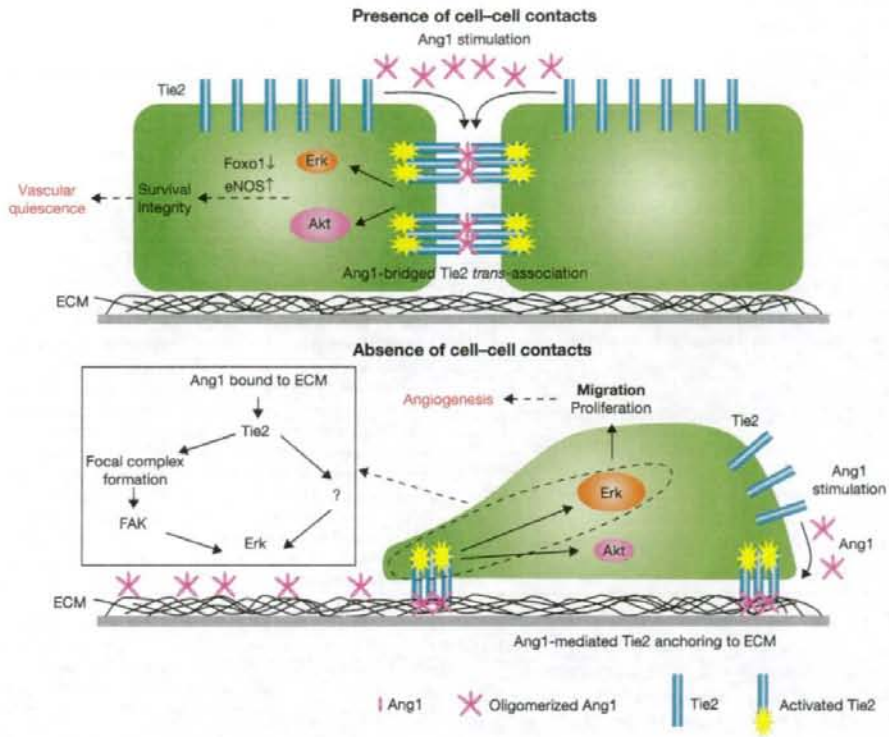

Figure 8 Schematic representation of a proposed model for how Ang1–Tie2 signalling is involved in both vascular quiescence and angiogenesis. (Upper panel) Under confluent conditions, oligomerized Ang1 bridges Tie2 at cell–cell contacts, resulting in formation of *trans*-association of Tie2. *Trans*-associated Tie2 at cell–cell contacts preferentially activates Akt–Foxo1 and Akt–eNOS signalling pathways, which may contribute to maintenance of vascular quiescence by enhancing endothelial survival and integrity (dashed arrows). (Lower panel) In the absence of cell–cell contacts, Tie2 forms a complex with ECM-bound Ang1 at cell–substratum contacts, which is different from focal adhesions, focal complexes and fibrillar adhesion. Ang1–Tie2 anchored to cell–substratum contacts preferentially activates the Erk pathway by inducing FAK-positive focal complex assembly. Ang1, therefore, seems to implicate FAK partly in the activation of Erk. This preferential activation of the Erk pathway induced by Ang1–Tie2 anchored to cell–substratum contacts may contribute to endothelial cell migration and proliferation, thereby promoting angiogenesis (dashed arrows). FC and ECM indicate focal complex and extracellular matrix, respectively.

The presence of cell–cell contacts determines preferential activation of Akt by Ang1 and subsequent phosphorylation of eNOS and Foxo1

Akt phosphorylates the forkhead transcription factor Foxo1 and endothelial nitric oxide synthase (eNOS), which play critical roles in endothelial functions[39,40]. To investigate the biological consequence of preferential activation of Akt by *trans*-associated Tie2, we examined Ang1-induced phosphorylation of Foxo1 and eNOS in the absence and presence of cell–cell contacts. Endothelial cell–cell contacts significantly enhanced COMP–Ang1-induced phosphorylation of Foxo1 and eNOS in HUVECs (Fig. 6a–c). Akt-dependent phosphorylation negatively regulates transcriptional activity of Foxo1 by promoting its nuclear exclusion. Consistently, nuclear export of Foxo1 by COMP–Ang1 was more prominent in confluent HUVECs than in sparse cells (Fig. 6d). Phosphatidylinositol-3 kinase (PI3K) inhibitor, LY294002, and Akt inhibitor impeded COMP–Ang1-induced phosphorylation of Foxo1 and eNOS (Fig. 6e, f). These findings indicate that phosphorylation of Foxo1 and eNOS mediated by PI3K–Akt are preferentially induced by *trans*-associated Tie2 compared to substratum-anchored Tie2.

Distinct gene expression profile in HUVECs upon Ang1 stimulation in the presence or absence of cell–cell contacts

To further clarify the consequence of Tie2 activation at cell–cell contacts and at cell–substratum contacts, we employed DNA microarray analyses. We carried out a global survey of mRNA in either confluent or sparse HUVECs upon COMP–Ang1 stimulation for 1 h. There was a striking difference in the induction of genes between confluent and sparse conditions (Fig. 7a). To confirm the microarray data, expression levels of several genes selectively induced under either sparse or confluent conditions were examined by quantitative real-time PCR analysis. Both basal expression and induction of *Krüppel-like factor (KLF) 10* and *suppressor of cytokine signaling 3* (*SOCS3*) were greater in sparse cells than in confluent cells (Fig. 7b, c). In contrast,

KLF2, zinc finger protein 36, C3H type 2 (TIS11d), and *connexin40* (*Cx40*) were induced by COMP–Ang1 selectively in confluent cells (Fig. 7d, e, f). *Cx40*, the product of which is involved in intercellular communication, is known to be repressed by Foxo1 in endothelial cells [39]. Indeed, overexpression of a constitutively active mutant of Foxo1 decreased *Cx40* expression (Fig. 7g). Thus, we investigated whether a PI3K–Akt–Foxo1 signal axis is involved in COMP–Ang1-induced *Cx40* expression. LY294002 and Akt inhibitor prevented COMP–Ang1-induced *Cx40* induction in confluent cells (Fig. 7h, i). Collectively, these microarray analyses and real-time PCR validation clearly demonstrate a difference in induction of gene expression by Ang1 in the presence or absence of cell–cell contacts, and indicate that *trans*-associated Tie2 at cell–cell contacts regulates Foxo1-dependent gene expression through preferential activation of Akt.

DISCUSSION

Localization of Tie2 upon Ang1 stimulation depends upon the presence or absence of cell–cell contacts (Figs 1a, 3a). Tie2 localization at cell–cell contacts appears to be due to Ang1-bridged Tie2 *trans*-association. Tie2 activation at cell–cell contacts resulted in preferential activation of Akt, which in turn led to inhibition of Foxo1-mediated gene regulation and phosphorylation of eNOS. The Akt–Foxo1 pathway is known to be involved in Ang1-induced endothelial cell survival and blood vessel stability[39]. It has been also reported that the Akt–eNOS pathway is required for vascular maturation[40]. Thus, *trans*-associated Tie2 may contribute to maintenance of vascular quiescence through the Akt–Foxo1 and Akt–eNOS signalling pathways.

Ang1 also locates Tie2 to cell–substratum contacts that are different from FCs, FAs and FBs and preferentially activates Erk in the absence of cell–cell contacts. This Tie2 localization was resistant to detergent[27,28], indicating Tie2 is anchored to cell–substratum contacts. Moreover, Ang1 could bind to ECM such as fibronectin and collagen, as previously reported[41,42]. Upon being anchored to ECM by Ang1, Tie2 activated Erk partly through FAK. Formation of the Ang1–Tie2 complex at cell–substratum contacts accelerated FC formation (Fig. 5b, e), and probably vice versa, resulting in the implicating FAK in Ang1-induced Erk activation in isolated cells. This notion is consistent with recent reports revealing a role for FAK in vascular development[43,44].

During angiogenesis, endothelial cells sprouting from the pre-existing blood vessels lose cell–cell adhesion and need to proliferate and migrate to form neovasculature. Erk is responsible for endothelial proliferation and migration during angiogenesis[38,45]. Inhibition of Erk resulted in decreased migration by substratum-anchored Ang1. As several lines of evidence suggest that Tie2 signalling mediates pathological and physiological angiogenesis[14,15,17–20], Ang1–Tie2–ECM complexes at cell–substratum contacts may accelerate angiogenesis by promoting proliferation and migration of isolated endothelial cells. However, regulation of angiogenesis by Ang1–Tie2 might be more complex, since it has been reported that Tie2 is expressed in stalk cells, but not in tip cells, which proliferate and migrate during angiogenesis[46]. Thus, further investigation is required to resolve this mechanism.

We propose that *trans*-associated Tie2 bridged by Ang1 and cell–substratum contact-anchored Tie2 by Ang1 might be preferable for vascular quiescence and for angiogenesis via Akt and Erk activation, respectively (Fig. 8). □

Note added in proof: a related manuscript by Saharinen et al. (Nature Cell Biol. ***10***, *527–537; doi:10.1038/ncb1715; 2008) is also published in this issue.*

METHODS

Immunocytochemistry and fluorescence imaging. HUVECs and CHO cells grown on a collagen-coated glass-base dish (Asahi Techno Glass Corporation, Chiba, Japan) were transfected with expression plasmids encoding Tie2–GFP, Tie2Δcyto–GFP, Tie2Δcyto–HA, RFP–Crk, GFP–tensin and RFP–FAT as indicated in the figures. HUVECs starved for 3 h in medium 199 containing 0.5% BSA and CHO cells in Dulbecco's modified Eagle's medium (DMEM)/F12 nutrient mixture (Sigma-Aldrich, St. Louis, MO) were stimulated for the time periods as indicated in the figures. After stimulation, the cells were fixed in PBS containing 2% formaldehyde for 30 min at 4 °C, washed with PBS, and permeabilized with 0.05% Triton X-100 for 30 min at 4 °C. To examine the detergent insolubility of Tie2–GFP anchoring to the substratum, the cells were washed with PBS, and extracted in 0.5% Triton X-100 in cytoskeleton stabilizing buffer containing 10 mM PIPES at pH 6.8, 300 mM sucrose, 100 mM NaCl, 3 mM $MgCl_2$, 1 mM EGTA and 1 x protease inhibitor cocktail (Roche Applied Science, Indianapolis, IN) for 3 min at room temperature (RT). After washing with PBS, the cells were fixed with 2% formaldehyde in PBS for 30 min at 4 °C. Cells were blocked with PBS containing 4% BSA for 1 h at RT and immunostained with anti-Tie2, anti-VE-cadherin, anti-HA, anti-FLAG, anti-vinculin, anti-α5 integrin, anti-β3 integrin, anti-PECAM-1, anti-VASP, anti-talin, anti-fibronectin, anti-phosphoTie2, and anti-FAK antibodies for 1 h at RT and with rhodamine-phalloidin for 20 min at RT. Protein reacting with antibody was visualized with species-matched Alexa 488- or Alexa 546-labelled secondary antibodies. Fluorescence images of GFP, RFP, rhodamine, Alexa 488 and Alexa 546 were recorded with an Olympus IX-81 inverted fluorescence microscope (Olympus Corporation, Tokyo, Japan) with a cooled CCD camera CoolSNAP-HQ (Roper Scientific, Tucson, AZ), and appropriate filter sets for GFP, Alexa 488 and Alexa 546, and with a FluoView FV1000 confocal microscope (Olympus Corporation) with a 60x oil immersion objective lens. HUVECs and CHO cells transfected with plasmids expressing fluorescently tagged proteins (GFP, HcRed, and RFP) were time-lapse imaged on an Olympus IX-81 inverted fluorescence microscope as described previously [47,48].

***In vitro* Ang1-bridged Tie2 association assay.** To produce recombinant sTie2–HA protein (extracellular domain of Tie2 tagged with HA), 293F cells were transfected with pcDNA3.1-sTie2–HA vector, and cultured in Free Style 293 expression media for 7 days. sTie2–HA protein secreted into the medium was collected every 2 days, and incubated with ProBond resin (Invitrogen Corp., Carlsbad, CA) overnight at 4 °C. sTie2–HA protein bound to the beads was eluted with 500 mM imidazole, concentrated with Amicon Centriplus (Millipore, Billerica, MA), and buffer exchanged into PBS by dialysis.

Ang1-bridged Tie2 association was analysed as described in Supplementary Information Fig. S3a. Initially, protein G sepharose beads (GE Healthcare Life Science, Piscataway, NJ) were incubated with 0.1 μg of Fc, sTie1–Fc or sTie2–Fc protein in binding buffer (50 mM Tris-HCl at pH 7.5, 100 mM NaCl, 0.02% Triton X-100) for 2 h at 4 °C, washed three times with binding buffer, and incubated with 1 μg of Ang1 or its variants (COMP–Ang1, GCN4–Ang1 and MAT–Ang1) for 2 h at 4 °C. The beads were extensively washed with binding buffer four times, and subsequently incubated with 3 μg of sTie2–HA protein for 2 h at 4 °C. After washing, the precipitates were subjected to Western blot analysis with anti-Flag and anti-HA antibodies to quantify the co-precipitated Ang1 and its variants and sTie2–HA protein, respectively. Proteins reacting with primary antibodies were visualized by the ECL system (GE Healthcare Life Science) for detecting peroxidase-conjugated secondary antibodies and analysed with an LAS-1000 system (Fuji Film, Tokyo, Japan).

Cell aggregation and *in vivo* Tie2 *trans*-association assays. Suspension 293F cells transfected with the plasmids expressing GFP, Tie2–GFP, Tie2Δcyto–GFP, Tie2KD–GFP, or VEGFR2 plus IRES-driven GFP were suspended in Free Style 293 expression media and placed on 6 well-plates in a density of 5.0×10^5 cells per well (1 ml per well). Then, the cells were agitated for 4 h using a gyratory shaker in the presence of vehicle, Ang1, COMP–Ang1 or VEGF. After the incubation, the phase-contrast and the fluorescence images were recorded by Olympus IX-81 inverted fluorescence microscope. The differential interference contrast (DIC) and the fluorescence images were also obtained with a FluoView

FV1000 confocal microscope. The numbers of cell aggregates including more than 4 cells were counted in, at least, 10 different fields. The size of cell aggregates was measured using MetaMorph 6.1 software.

For the *in vivo* Tie2 *trans*-association assay, 293F cells transfected with the vectors encoding either GFP, Tie2Δcyto–GFP, or Tie2Δcyto–HA were washed and resuspended in DMEM in a density of 10^6 cells per ml. The cells expressing Tie2Δcyto–HA were mixed with either those expressing Tie2Δcyto–GFP or those expressing GFP in a 6 well-plate (2×10^6 cells $well^{-1}$). The cell suspensions were agitated for 1 h in the presence or absence of 400 ng ml^{-1} COMP–Ang1. After the incubation, the cells were collected in a 15 ml-conical tube, washed with ice-cold PBS and lysed at 4°C in lysis buffer containing 50 mM Tris-HCl at pH 7.5, 150 mM NaCl, 0.5% Triton X-100 and 1 x protease inhibitor cocktail. BaF–Tie2Δcyto–HA cells (1.5×10^6 cells) were also mixed with either BaF3 cells (1.5×10^6 cells) or BaF–Tie2Δcyto–GFP cells (1.5×10^6 cells) in RPMI1640 (Nissui, Tokyo, Japan) supplemented with 2 ng ml^{-1} murine IL3, and stimulated with or without 400 ng ml^{-1} COMP–Ang1 for 5 h. After the incubation, the cells were washed with ice-cold PBS and lysed as described above. Precleared cell lysates were subjected to immunoprecipitaion with anti-GFP antibody followed by immunoblot analysis with anti-HA antibody.

Microarray analysis. Confluent and sparse HUVECs on a collagen-coated dish were starved in HuMedia-EB2 medium (Kurabo, Kurashiki, Japan) containing 0.5% fetal calf serum (FCS) for 15 h, and stimulated with vehicle or COMP–Ang1 (200 ng ml^{-1}) for 1 h. After the stimulation, total RNAs were purified from the pooled RNA of triplicate samples using Trizol reagent (Invitrogen Corp.) and reverse-transcribed to cDNAs. Biotin-labelled RNAs derived from cDNAs were fragmented according to the manufacturer's instructions (Affymetrix, Santa Clara, CA). Labelled cRNA probes were hybridized to Affymerix U133plus 2.0 array (Affymetrix). The microarray data scanned through an Affymetrix GeneChip scanner 3000 7G were globally normalized by Affymetrix Microarray Suite 5.0 software and were scaled to a target intensity of 100. Microarray analysis was performed in duplicate from independent RNA preparations. Data were analysed according to the minimum information about a microarray experiment (MIAME) rule. To identify the genes regulated by Ang1–Tie2 signal, we picked up the genes which fulfill the two criteria: (1) the hybridization signal after COMP–Ang1 stimulation was higher than 80 in duplicate experiments and (2) the induction was greater than 1.5-fold under either confluent or sparse conditions upon COMP–Ang1 stimulation in duplicate experiments. The genes that conformed to the two criteria were further clustered on the basis of similar regulation patterns using Gene cluster (created by M. B. Eisen, University od California, Berkeley, CA) and Java Tree View software according to the manual on the default settings. The complete microarray data sets are available from the Gene Expression Omnibus (GSE9677).

Note: Supplementary Information is available on the Nature Cell Biology website.

ACKNOWLEDGEMENTS

We are grateful to T. Suda (Keio University, Tokyo, Japan) for the Tie2 cDNA, to A. Fukamizu (University of Tsukuba, Tsukuba, Japan) for the Foxo1 cDNA, to K.M. Yamada (National Institute of Health) for GFP–tensin, to J. Nakae (Kobe University Graduate School of Medicine, Kobe, Japan) for the adenovirus encoding Foxo1 mutant, to A. Mizushima, M. Sone, M. Maeoka, and Y. Matsuura for technical assistance, to M. Masuda, H. Hanada, and S. Yamanoto for helpful advice and to J.T. Pearson and J.S. Gutkind for critical reading of the manuscript. This work was supported in part by grants from the Ministry of Education, Science, Sports and Culture of Japan; the Ministry of Health, Labour, and Welfare of Japan; and the Program for the Promotion of Fundamental Studies in Health Sciences of the National Institute of Biomedical Innovation (to S.F., T.M, T.K. N.M.); the Naito Foundation (to S.F.); Takeda Medical Research Foundation (to N.M); and KOSEF through the NRL Program (2004-02376 to G.Y.K) funded by the MOST.

AUTHOR CONTRIBUTIONS

S. F. and N. M. designed and wrote the paper. S. F. performed the all cell biological and biochemical analysis. K. S. and K. N. helped with the experiments performed by S. F. T. M. and T. K. performed microarray analyses. M. S. and N. T. helped with VEGF-related and Tie2–BaF experiments. H. Z. K. and G. Y. K. prepared several forms of recombinant Ang1.

COMPETING FINANCIAL INTERESTS

The authors declare no competing financial interests.

Published online at http://www.nature.com/naturecellbiology/
Reprints and permissions information is available online at http://npg.nature.com/reprintsandpermissions/

1. Yancopoulos, G. D. *et al.* Vascular-specific growth factors and blood vessel formation. *Nature* **407,** 242–248 (2000).
2. Mammoto, T. *et al.* Angiopoietin-1 requires p190RhoGAP to protect against vascular leakage *in vivo*. *J. Biol. Chem.* **282,** 23910–23918 (2007).
3. Jho, D. *et al.* Angiopoietin-1 opposes VEGF-induced increase in endothelial permeability by inhibiting TRPC1-dependent Ca2 influx. *Circ. Res.* **96,** 1282–1290 (2005).
4. Brindle, N. P., Saharinen, P. & Alitalo, K. Signaling and functions of angiopoietin-1 in vascular protection. *Circ. Res.* **98,** 1014–1023 (2006).
5. Baffert, F., Le, T., Thurston, G. & McDonald, D. M. Angiopoietin-1 decreases plasma leakage by reducing number and size of endothelial gaps in venules. *Am. J. Physiol. Heart Circ. Physiol.* **290,** H107-H118 (2005).
6. Gamble, J. R. *et al.* Angiopoietin-1 is an antipermeability and anti-inflammatory agent *in vitro* and targets cell junctions. *Circ. Res.* **87,** 603–607 (2000).
7. Cho, C. H. *et al.* Designed angiopoietin-1 variant, COMP-Ang1, protects against radiation-induced endothelial cell apoptosis. *Proc. Natl Acad. Sci.USA* **101,** 5553–5558 (2004).
8. Kwak, H. J., So, J. N., Lee, S. J., Kim, I. & Koh, G. Y. Angiopoietin-1 is an apoptosis survival factor for endothelial cells. *FEBS Lett.* **448,** 249–253 (1999).
9. Papapetropoulos, A. *et al.* Angiopoietin-1 inhibits endothelial cell apoptosis via the Akt/Survivin pathway. *J. Biol. Chem.* **275,** 9102–9105 (2000).
10. Thurston, G. *et al.* Angiopoietin-1 protects the adult vasculature against plasma leakage. *Nature Med.* **6,** 460–463 (2000).
11. Thurston, G. *et al.* Leakage-resistant blood vessels in mice transgenically overexpressing angiopoietin-1. *Science* **286,** 2511–2514 (1999).
12. Master, Z. *et al.* Dok-R plays a pivotal role in angiopoietin-1-dependent cell migration through recruitment and activation of Pak. *EMBO J.* **20,** 5919–5928 (2001).
13. Kim, I. *et al.* Angiopoietin-1 induces endothelial cell sprouting through the activation of focal adhesion kinase and plasmin secretion. *Circ. Res.* **86,** 952–959 (2000).
14. Cho, C. H. *et al.* COMP-Ang1: A designed angiopoietin-1 variant with nonleaky angiogenic activity. *Proc. Natl Acad. Sci. USA* **101,** 5547–5552 (2004).
15. Asahara, T. *et al.* Tie2 receptor ligands, angiopoietin-1 and angiopoietin-2, modulate VEGF-induced postnatal neovascularization. *Circ. Res.* **83,** 233–240 (1998).
16. Yoon, M. J. *et al.* Localization of Tie2 and phospholipase D in endothelial caveolae is involved in angiopoietin-1-induced MEK/ERK phosphorylation and migration in endothelial cells. *Biochem. Biophys. Res. Commun.* **308,** 101–105 (2003).
17. Lin, P. *et al.* Inhibition of tumor angiogenesis using a soluble receptor establishes a role for Tie2 in pathologic vascular growth. *J. Clin. Invest.* **100,** 2072–2078 (1997).
18. Lin, P. *et al.* Antiangiogenic gene therapy targeting the endothelium-specific receptor tyrosine kinase Tie2. *Proc. Natl Acad. Sci. USA* **95,** 8829–8834 (1998).
19. Peters, K. G. *et al.* Functional significance of Tie2 signaling in the adult vasculature. *Recent Prog. Horm. Res.* **59,** 51–71 (2004).
20. Wong, A. L. *et al.* Tie2 expression and phosphorylation in angiogenic and quiescent adult tissues. *Circ. Res.* **81,** 567–574 (1997).
21. Carmeliet, P. *et al.* Targeted deficiency or cytosolic truncation of the VE-cadherin gene in mice impairs VEGF-mediated endothelial survival and angiogenesis. *Cell* **98,** 147–157 (1999).
22. Zanetti, A. *et al.* Vascular endothelial growth factor induces SHC association with vascular endothelial cadherin: a potential feedback mechanism to control vascular endothelial growth factor receptor-2 signaling. *Arterioscler. Thromb. Vasc. Biol.* **22,** 617–622 (2002).
23. Lampugnani, M. G., Orsenigo, F., Gagliani, M. C., Tacchetti, C. & Dejana, E. Vascular endothelial cadherin controls VEGFR-2 internalization and signaling from intracellular compartments. *J. Cell Biol.* **174,** 593–604 (2006).
24. Zaidel-Bar, R., Cohen, M., Addadi, L. & Geiger, B. Hierarchical assembly of cell-matrix adhesion complexes. *Biochem. Soc. Trans.* **32,** 416–420 (2004).
25. Geiger, B., Bershadsky, A., Pankov, R. & Yamada, K. M. Transmembrane crosstalk between the extracellular matrix–cytoskeleton crosstalk. *Nature Rev. Mol. Cell Biol* **2,** 793–805 (2001).
26. Cascone, I., Napione, L., Maniero, F., Serini, G. & Bussolino, F. Stable interaction between α5β1 integrin and Tie2 tyrosine kinase receptor regulates endothelial cell response to Ang-1. *J. Cell Biol.* **170,** 993–1004 (2005).
27. Wulfkuhle, J. D. *et al.* Domain analysis of supervillin, an F-actin bundling plasma membrane protein with functional nuclear localization signals. *J. Cell Sci.* **112,** 2125–2136 (1999).
28. Adams, C. L., Nelson, W. J. & Smith, S. J. Quantitative analysis of cadherin-catenin-actin reorganization during development of cell-cell adhesion. *J. Cell Biol.* **135,** 1899–1911 (1996).
29. Kim, I. *et al.* Angiopoietin-1 regulates endothelial cell survival through the phosphatidylinositol 3'-Kinase/Akt signal transduction pathway. *Circ. Res.* **86,** 24–29 (2000).
30. Kanda, S., Miyata, Y., Mochizuki, Y., Matsuyama, T. & Kanetake, H. Angiopoietin 1 is mitogenic for cultured endothelial cells. *Cancer Res.* **65,** 6820–6827 (2005).
31. Teichert-Kuliszewska, K. *et al.* Biological action of angiopoietin-2 in a fibrin matrix model of angiogenesis is associated with activation of Tie2. *Cardiovasc. Res.* **49,** 659–670 (2001).
32. Weber, C. C. *et al.* Effects of protein and gene transfer of the angiopoietin-1 fibrinogen-like receptor-binding domain on endothelial and vessel organization. *J. Biol. Chem.* **280,** 22445–22453 (2005).

33. Dallabrida, S. M., Ismail, N., Oberle, J. R., Himes, B. E. & Rupnick, M. A. Angiopoietin-1 promotes cardiac and skeletal myocyte survival through integrins. *Circ. Res.* **96,** e8-24 (2005).
34. Aplin, A. E., Short, S. M. & Juliano, R. L. Anchorage-dependent regulation of the mitogen-activated protein kinase cascade by growth factors is supported by a variety of integrin α chains. *J. Biol. Chem.* **274,** 31223–31228 (1999).
35. Short, S. M., Talbott, G. A. & Juliano, R. L. Integrin-mediated signaling events in human endothelial cells. *Mol. Biol. Cell* **9,** 1969–1980 (1998).
36. Schlaepfer, D. D. & Mitra, S. K. Multiple connections link FAK to cell motility and invasion. *Curr. Opin. Genet. Dev.* **14,** 92–101 (2004).
37. Parsons, J. T. Focal adhesion kinase: the first ten years. *J. Cell Sci.* **116,** 1409–1416 (2003).
38. Eliceiri, B. P., Klemke, R., Stromblad, S., & Cheresh, D. A. Integrin αV β3 requirement for sustained mitogen-activated protein kinase activity during angiogenesis. *J. Cell Biol.* **140,** 1255–1263 (1998).
39. Daly, C. *et al.* Angiopoietin-1 modulates endothelial cell function and gene expression via the transcription factor FKHR (FOXO1). *Genes Dev.* **18,** 1060–1071 (2004).
40. Chen, J. *et al.* Akt1 regulates pathological angiogenesis, vascular maturation and permeability in vivo. *Nature Med.* **11,** 1188–1196 (2005).
41. Xu, Y. & Yu, Q. Angiopoietin-1, unlike angiopoietin-2, is incorporated into the extracellular matrix via its linker peptide region. *J. Biol. Chem.* **276,** 34990–34998 (2001).
42. Carlson, T. R., Feng, Y., Maisonpierre, P. C., Mrksich, M. & Morla, A. O. Direct cell adhesion to the angiopoietins mediated by integrins. *J. Biol. Chem.* **276,** 26516–26525 (2001).
43. Braren, R. *et al.* Endothelial FAK is essential for vascular network stability, cell survival, and lamellipodial formation. *J. Cell Biol.* **172,** 151–162 (2006).
44. Shen, T. L. *et al.* Conditional knockout of focal adhesion kinase in endothelial cells reveals its role in angiogenesis and vascular development in late embryogenesis. *J. Cell Biol.* **169,** 941–952 (2005).
45. Meadows, K. N., Bryant, P. & Pumiglia, K. Vascular endothelial growth factor induction of the angiogenic phenotype requires Ras activation. *J. Biol. Chem.* **276,** 49289–49298 (2001).
46. Yana, I. *et al.* Crosstalk between neovessels and mural cells directs the site-specific expression of MT1-MMP to endothelial tip cells. *J. Cell Sci.* **120,** 1607–1614 (2007).
47. Nagashima, K. *et al.* Adaptor protein Crk is required for ephrin-B1-induced membrane ruffling and focal complex assembly of human aortic endothelial cells. *Mol. Biol. Cell* **13,** 4231–4242 (2002).
48. Sakurai, A. *et al.* MAGI-1 is required for Rap1 activation upon cell-cell contact and for enhancement of vascular endothelial cadherin-mediated cell adhesion. *Mol. Biol. Cell* **17,** 966–976 (2006).

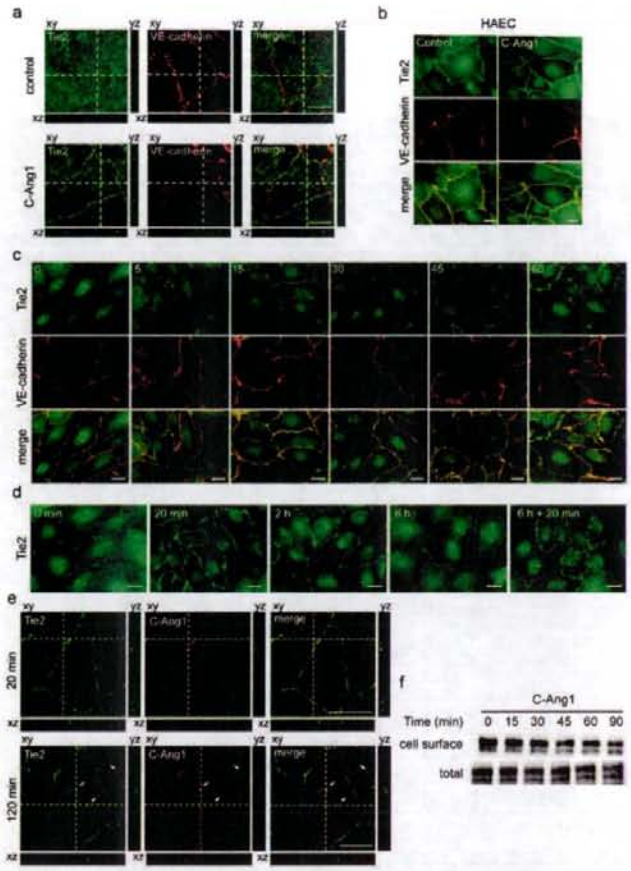

Figure S1 Tie2 accumulate at endothelial cell-cell contacts. **(a)** Confluent HUVECs plated on collagen-coated glass-base dish were starved in medium 199 containing 0.5% BSA for 3 h and stimulated with vehicle (control) or 200 ng ml^{-1} COMP-Ang1 (C-Ang1) for 20 min. The cells were then fixed, immunostained with anti-Tie2 and anti-VE-cadherin antibodies, and visualised with Alexa 488- and Alexa 546-conjugated secondary antibodies. Optical sections of Alexa 488 (green) and Alexa 546 (red) images were obtained by an FV-1000 confocal laser scanning microscope (Olympus). The bottom and the right panels of each image show *xz* section and *yz* section at x line and y line (white broken lines) of the *xy* image. Images for immunostaining of anti-Tie2 and anti-VE-cadherin antibodies are merged (merge). **(b)** Confluent human aortic endothelial cells (HAECs) were stimulated with vehicle (control) or COMP-Ang1 (C-Ang1) and imaged similar to **a** using an Olympus IX-81 epifluorescent microscope instead of a confocal microscope. **(c)** Confluent HUVECs stimulated with COMP-Ang1 for the time (min) indicated on the top panels were immunostained with anti-Tie2 and anti-VE-cadherin antibodies, and visualised similarly to **b**. **(d)** Confluent HUVECs were stimulated with COMP-Ang1 for the time indicated on the top panels, and stained with anti-Tie2 antibody similarly to **b**. In right panel, the cells exposed to COMP-Ang1 for 6 h were re-challenged with COMP-Ang1 for 20 min (6 h + 20 min). **(e)** Confluent HUVECs stimulated with COMP-Ang1 for 20 min (top panels) and 120 min (bottom panels) were stained with anti-Tie2 and anti-Flag antibodies, and visualised with Alexa 488- and Alexa 546-conjugated secondary antibodies, respectively. Optical sections of Alexa 488 (green; Tie2) and Alexa 546 (red; C-Ang1) images were obtained as described in the legend of **a**. The bottom and the right panels of each image show *xz* section and *yz* section at x line and y line (white broken lines) of the *xy* image. Images for immunostaining of anti-Tie2 and anti-Flag antibodies are merged (right column; merge). **(f)** Confluent HUVECs were stimulated with COMP-Ang1 for the time (min) indicated at the top. After the stimulation, cell-surface (upper panel) and total (bottom panel) expression level of Tie2 was quantified by biotinylation assay as described in Supplementary Methods. **(g)** Confluent HUVECs plated on collagen-coated glass-base dish were transfected with the plasmid encoding Tie2-GFP and that encoding HcRed-p120 catenin, starved for 3 h, and stimulated with 200 ng ml^{-1} COMP-Ang1. Tie2-GFP and HcRed-p120 catenin were time-lapse imaged on Olympus IX-81 inverted fluorescence microscope. A series of GFP and HcRed images were collected by MetaMorph 6.1 software. Images of GFP (top) and HcRed (middle) at the time points (min) indicated on the top panels after COMP-Ang1 stimulation were shown. Merged images are also shown at the bottom. **(h)** Confluent HUVECs transfected with the plasmid encoding Tie2-GFP was starved and stimulated with either vehicle (control; top panels) or COMP-Ang1 (C-Ang1; bottom panels) for 30 min. After the stimulation, the cells were stained with anti-VE-cadherin antibody and visualised by Alexa 546-conjugated secondary antibody as described in the legend of **b**. Images of GFP (green), Alexa 546 (red), and the merged images are shown at the left, middle, and right columns, respectively. The boxed areas are enlarged beneath each image. The scale bars represent 20 μm (a-e, g, h).

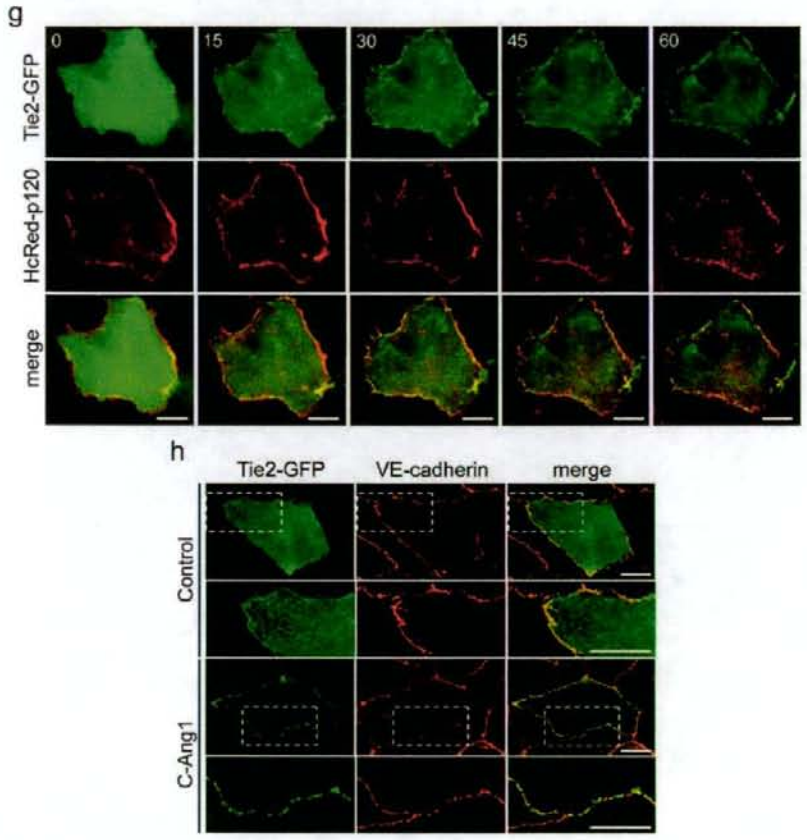

Figure S1 Continued

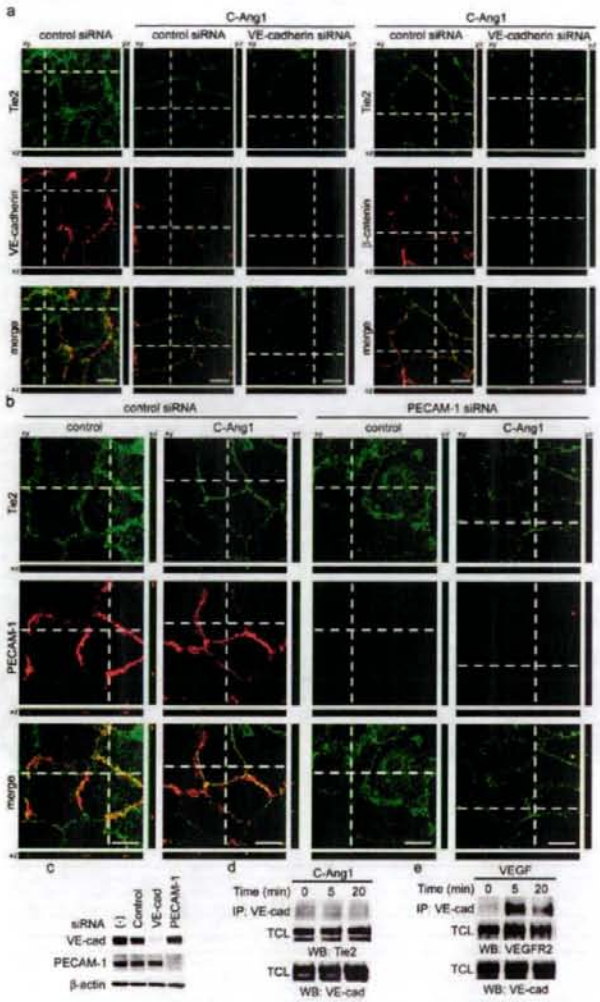

Figure S2 Translocation of Tie2 at cell-cell contacts does not require VE-cadherin and PECAM-1, but depends upon the expression of Tie2 on the neighbouring cells. **(a)** HUVECs transfected with control small interfering RNAs (siRNAs) or VE-cadherin siRNAs as indicated at the top were replated on the collagen-coated glass-base dish. The cells were stimulated with vehicle (most left column) or 200 ng ml^{-1} COMP-Ang1 (C-Ang1: from second column to fifth column), fixed, and immunostained with anti-Tie2 (top) and anti-VE-cadherin (middle) antibodies (from the first column to third column) and with anti-Tie2 (top) and anti-β-catenin (middle) antibodies (the fourth and fifth column, respectively), similarly to **Fig. S1a**. Merged images are shown at the bottom (merge). Note that depletion of VE-cadherin inhibits the accumulation of β-cateinin but not Tie2 at cell-cell contacts. **(b)** Similarly to **a**, HUVECs transfected with either control siRNAs or platelet and endothelial adhesion molecule-1 (PECAM-1) siRNAs were stimulated with vehicle (control) or COMP-Ang1 (C-Ang1), and immunostained with anti-Tie2 (top) and anti-PECAM-1 (middle) antibodies. Merged images are shown at the bottom (merge). Note that accumulation of Tie2 at cell-cell contacts was not affected by depletion of PECAM-1. **(c)** The cell lysates from HUVECs transfected without (-) or with control, VE-cadherin (VE-cad), or PECAM-1 siRNAs were subjected to SDS-PAGE followed by immunoblotting with antibodies as indicated at the left. We used two kinds of siRNAs for VE-cadherin and PECAM-1. Representative results obtained from one siRNA for each target are shown (a, b, and c), as described in the Supplementary Methods. **(d, e)** VEGFR2 but not Tie2 associates with VE-cadherin upon ligand stimulation. The cell lysates from HUVECs stimulated with COMP-Ang1 (d) or VEGF (e) for the time (min) indicated at the top were immunoprecipitaed with anti-VE-cadherin antibody. Total cell lysates (TCL) and immunoprecipitates were subjected to SDS-PAGE followed by immunoblotting with antibodies indicated at the bottom. **(f)** CHO cells expressing Tie2-GFP were stimulated with vehicle (control) or COMP-Ang1 (C-Ang1) for 20 min and optically sectioned for GFP images using a confocal microscope similarly to **Fig. S1a**. Note that Tie2-GFP, homogenously expressed on the plasma membrane before stimulation, was targeted to cell-cell contacts by COMP-Ang1 stimulation, as revealed in *xz* and *yz* sections. **(g)** CHO cells expressing either Tie2-GFP, Tie2Δcyto-GFP, or Tie2KD-GFP surrounded by wild type CHO cells were stimulated with vehicle (control) or COMP-Ang1 (C-Ang1). Note that Tie-GFP but not Tie2Δcyto-GFP and Tie2KD-GFP was internalised upon COMP-Ang1 stimulation, suggesting that *trans*-association of Tie2 at cell-cell contacts prevents Tie2 from internalisation and that kinase activity of Tie2 is required for internalisation of Tie2. The scale bars represent 20 μm (a, b, f, g).

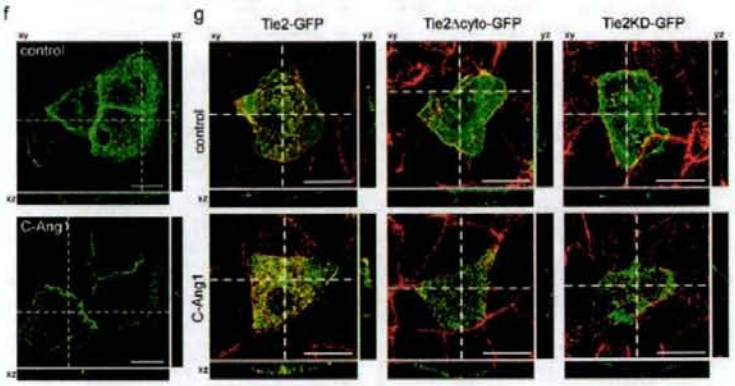

Figure S2 Continued

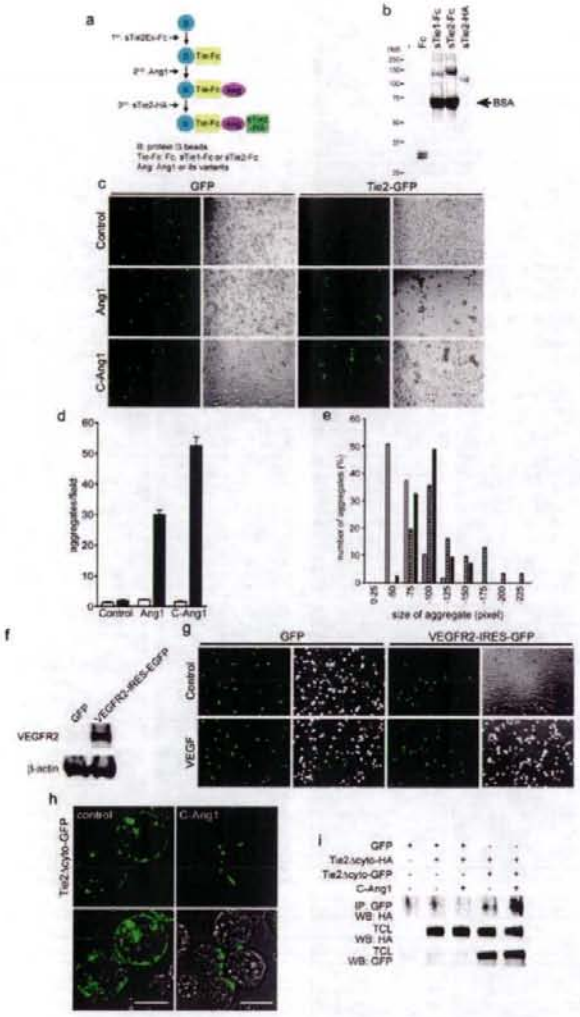

Figure S3 Ang1 induces *trans*-association of Tie2 at cell-cell contacts. **(a)** Schematic illustration of the experiment for in vitro Ang1-bridged Tie2 association assay. Detail of the assay protocol is described in Methods. **(b)** SDS-PAGE and coomassie staining confirmed the purity of the proteins used for Ang1-bridged Tie2 association assay. Arrow indicates BSA. **(c)** Aggregation of suspension 293F cells expressing GFP (left panels) and Tie2-GFP (right panels) was induced by either vehicle (control; top panels), Ang1 (Ang1; middle panels), and COMP-Ang1 (C-Ang1; bottom panels), as described in Methods. Left and right images of the panels show the GFP and the phase-contrast images, respectively. **(d)** To quantify the cell aggregation observed in **c**, the number of cell aggregate per field of microscopic view was counted. Aggregate was defined as cell mass consisting of more than 4 cells. The number of aggregate of the cells expressing GFP and Tie2-GFP was shown as white and black columns, respectively. Data are expressed as mean number ± standard deviation of, at least, ten different fields. **(e)** In the 293F cell aggregation assay described in **Fig. 2d**, the size of aggregate of the cells stimulated with COMP-Ang1 was measured using MetaMorph 6.1 software. Open, hatched and closed columns indicate the number of aggregate of the cells expressing Tie2-GFP, Tie2Δcyto-GFP and Tie2KD-GFP, respectively. **(f)** The lysates from cells expressing GFP and cells expressing both VEGFR2 and IRES-driven GFP were subjected to immunoblot analysis with antibodies indicated at the left. **(g)** Aggregation of 293F cells expressing GFP (left panels) and those expressing both VEGFR2 and IRES-driven GFP (right panels) was induced by either vehicle (control; top panels) and VEGF (VEGF; bottom panels), as described in the legend of **c**. Note that neither 293F cells expressing GFP nor 293F cells expressing VEGFR2 and IRES-driven GFP did not aggregate upon VEGF stimulation. **(h)** BaF3 cells expressing Tie2Δcyto-GFP (BaF-Tie2Δcyto-GFP) were incubated with vehicle (control; left column) and COMP-Ang1 (C-Ang1; right column) in suspension, as described in the legend of **Fig. 2f**. GFP and DIC images were obtained through a confocal microscope. Upper and lower panels show the GFP images merged without or with the DIC images, respectively. Note that Tie2Δcyto-GFP clearly localises at the site of cell-cell contacts only when stimulated with COMP-Ang1. The scale bars represent 10 μm. **(i)** BaF-Tie2Δcyto-HA cells (Tie2Δcyto-HA) were mixed-cultured with either BaF3 cells or BaF-Tie2Δcyto-GFP cells (Tie2Δcyto-GFP), and stimulated with 400 ng ml^{-1} of COMP-Ang1 for 5 h. Cell lysates were immunoprecipitated with anti-GFP antibody. Immunoprecipitates (IP) and aliquots of cell lysate (TCL) were subjected to Western blot analysis (WB) with anti-HA and anti-GFP antibodies as indicated at the left of each panel. Note that Tie2Δcyto-HA is coimmunoprecipitated with Tie2Δcyto-GFP upon COMP-Ang1 stimulation.

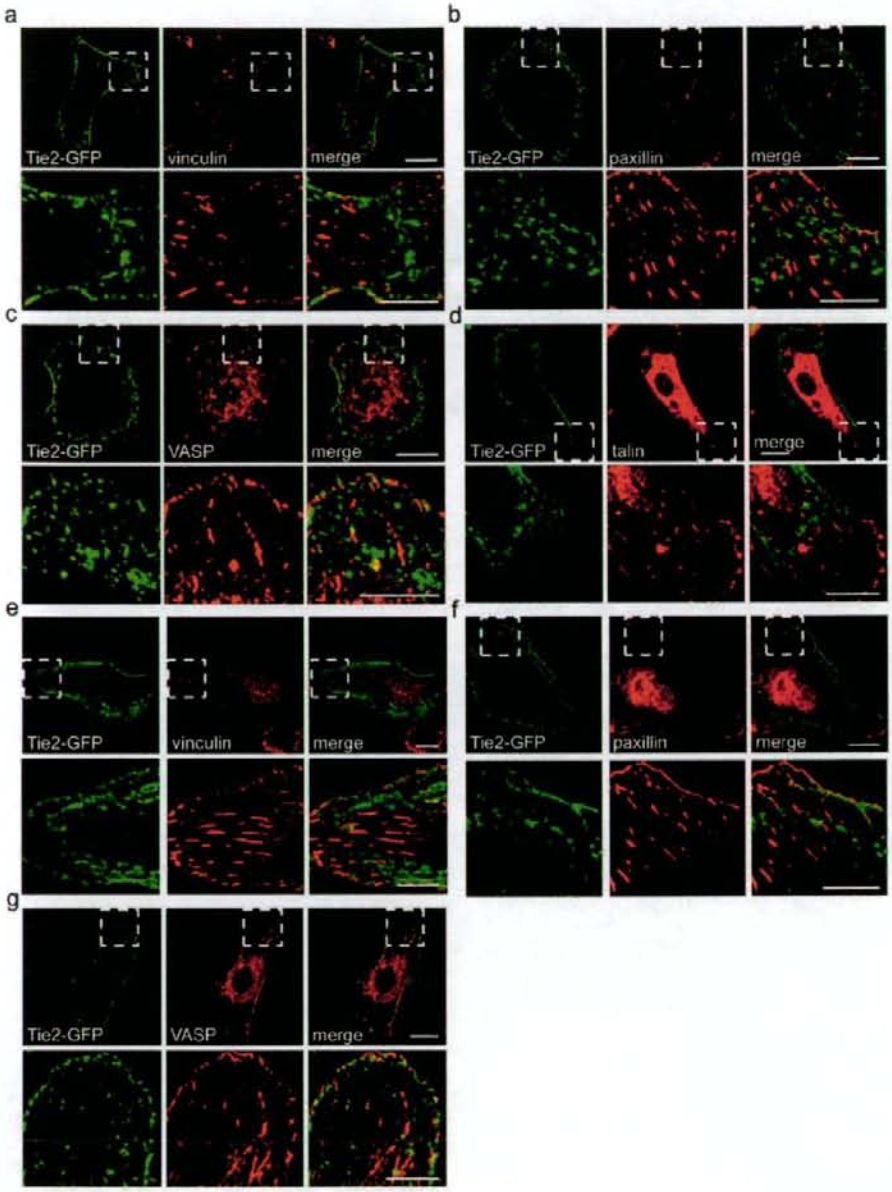

Figure S4 Tie2 accumulates to cell-substratum contacts upon Ang1 stimulation. **(a)** Subconfluent HUVECs were stimulated with vehicle (control) or COMP-Ang1 (C-Ang1) for 20 min, immunostained after fixation, and imaged similarly to **Fig. S1b**. As far as cells contact neighboring cells, Tie2 accumulates at cell-cell contacts upon Ang1 stimulation. **(b)** Isolated HUVECs stimulated with either vehicle (control; top panels), COMP-Ang1 (C-Ang1; middle panels) or native Ang1 (Ang1; bottom panels) for 20 min were fixed, immunostained with anti-Tie2 and anti-paxillin antibodies, and optically sectioned by a laser confocal microscope as in the legend of **Fig. S1a**. Merged images of Tie2 and paxillin are stacked and shown at the left column (stacked image). The sections at the bottom of the cell are shown (basal surface). The boxed region is enlarged at the right (enlargement). Note that Tie2 diffusely expressed on the bottom is relocated to the cell periphery at the bottom after COMP-Ang1 and native Ang1 stimulation. In addition, the peripheral accumulation at the bottom of the cells does not colocalise to paxillin-positive focal complexes, although Tie2 and paxillin expression partially overlap. **(c)** Images at the time point (30 min) of **Fig. 3b** are shown again and the boxed regions are enlarged at the bottom. Note that Tie2-GFP expressed in CHO cells does not colocalise with vinculin-positive focal complexes and focal adhesions. The scale bars represent 20 μm (a-c). The scale bars in the enlarged images represent 5 μm (a-c).

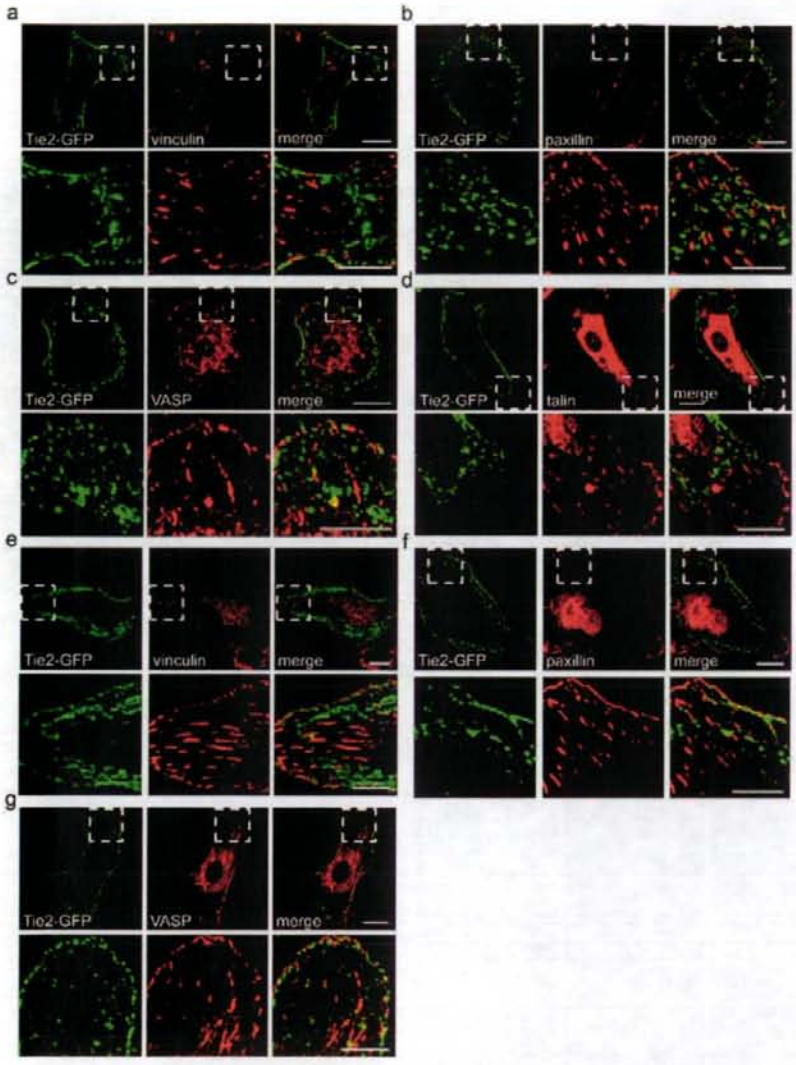

Figure S5 Tie2 accumulates to cell-substratum contacts distinct from focal complexes, focal adhesions, and fibrillar adhesions upon Ang1 stimulation. **(a-d)** Sparse HUVECs plated on fibronectin-coated dish were transfected with the plasmid encoding Tie2-GFP, and stimulated with COMP-Ang1 for 20 min. After fixation, the cells were stained with either anti-vinculin (**a**), anti-paxillin (**b**), anti-VASP (**c**), or anti-talin (**d**) antibodies, and visualized with Alexa546-labeled secondary antibodies. GFP (left panels) and Alexa546 (middle panels) images at cell-substratum interface were obtained by an FV1000 confocal laser scanning microscope. Merged images are shown at the right panels. The boxed regions are enlarged at the bottom of each image. (**e-g**) Tie2-GFP-expressing HUVECs plated on collagen-coated dish were stimulated as described in the legend of **a**, and stained with either anti-vinculin (**e**), anti-paxillin (**f**) or anti-VASP (**g**) antibodies, and visualized with Alexa546-labeled secondary antibodies. GFP and Alexa546 images at cell-substratum interface were obtained and shown similarly to **a**. (**h, i**) Sparse HUVECs plated on fibronectin-coated dish were transfected with the plasmid encoding Tie2-GFP, and stimulated with vehicle (control; left columns) or COMP-Ang1 (C-Ang1; middle and right columns) for 20 min. After fixation, the cells were stained with either anti-α5 integrin (**h**) or anti-fibronectin antibody (**i**), and visualized with Alexa546-conjugated secondary antibody. GFP (Tie2-GFP; top panels) and Alexa546 (α5 integrin or fibronectin; middle panels) images at cell-substratum interface were obtained by an FV1000 confocal laser scanning microscope. Merged images are shown at the bottom. The boxed regions are enlarged at the right of each image. (**j**) Sparse HUVECs plated on fibronectin-coated dish were co-transfected with the plasmid encoding Tie2-HA and that expressing GFP-tensin, and stimulated similarly to the legend of **h**. After fixation, the cells were stained with anti-HA antibody, and visualized with Alexa546-conjugated secondary antibody. Alexa546 (Tie2-HA; top panels) and GFP (GFP-tensin; middle panels) images at cell-substratum interface were recorded and shown as described in the legend of **h**. The scale bars represent 20 μm (a-j). The scale bars in the enlarged images represent 10 μm (a-j). Note that Tie2-GFP or Tie2-HA at cell-substratum contacts does not colocalise with markers for focal complexes, focal adhesions, and fibrillar adhesions.

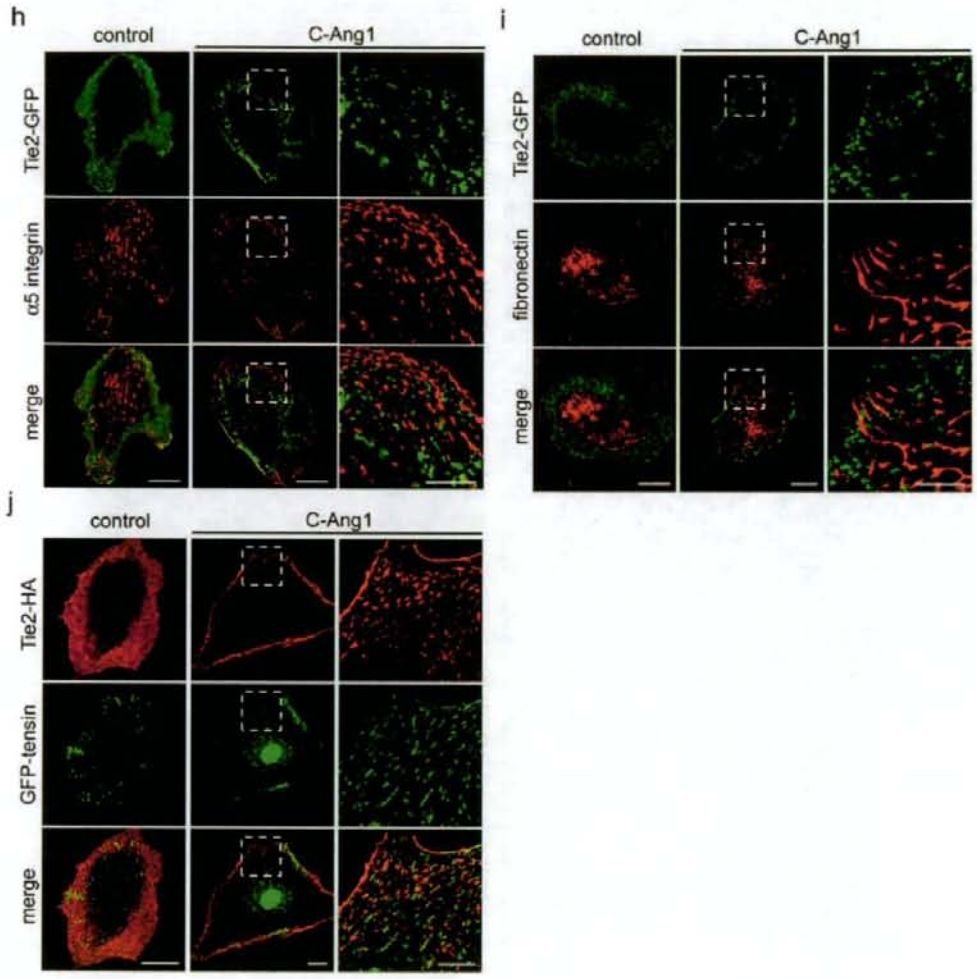

Figure S5 Continued

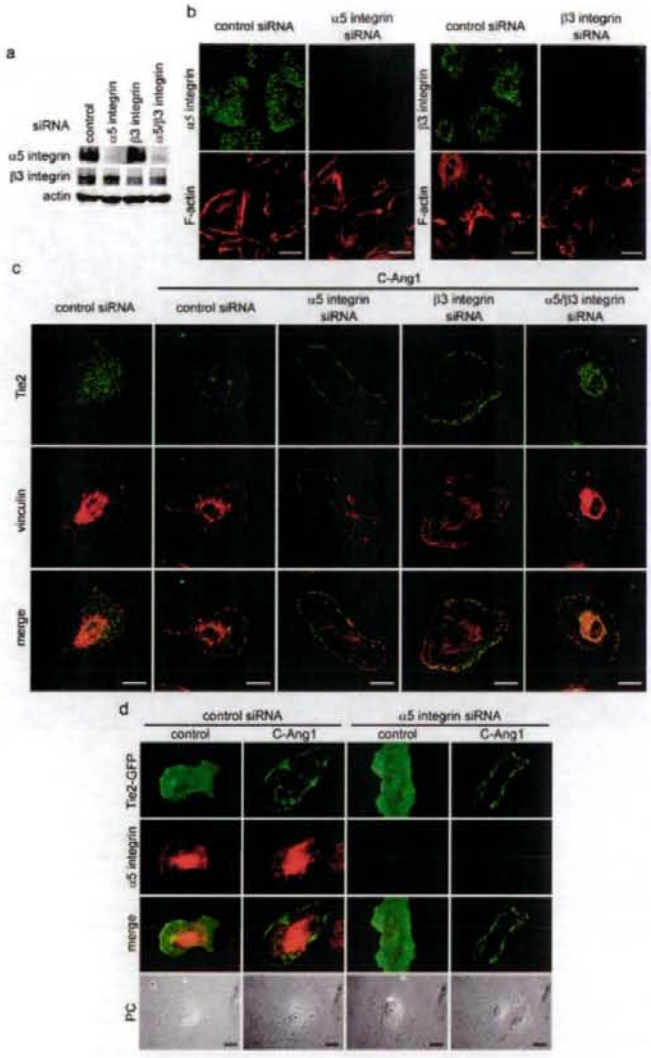

Figure S6. Depletion of α5 or β3 integrin does not affect the anchoring of Tie2 to cell-substratum contacts. **(a)** Cell lysates from HUVECs transfected with siRNAs indicated at the top for 24 h were subjected to immunoblot analysis using antibodies indicated at the left. **(b)** HUVECs transfected with siRNAs indicated at the top were immunostained with anti-α5 integrin (left) and anti-β3 integrin (right) and optically sectioned similarly to **Fig. S1a.** The sections of the bottom of the cells were shown. Cells were identified by F-actin staining using rhodamine-phalloidin. A representative result from more than 100 cells observed at one of three independent experiments is shown. **(c)** Isolated HUVECs transfected with siRNAs indicated at the top were unstimulated (control; first column) or stimulated with COMP-Ang1 (C-Ang1), followed by the immunostaining with anti-Tie2 (top) and anti-vinculin (middle) antibodies, and optically sectioned similarly to **Fig. S1a**. The sections at the bottom of the cells are shown. Merged images are shown at bottom. Note that COMP-Ang1-induced accumulation of Tie2 at cell-substratum contacts of the cell periphery was not affected by depletion of α5 and β3 integrins. **(d)** HUVECs transfected with control or α5 integrin siRNAs cultured for 24 h were replated on collagen-coated glass base dish. Cells were further transfected with the plasmid expressing Tie2-GFP, starved for 3 h, and stimulated with vehicle (control) and 200 ng ml^{-1} COMP-Ang1 (C-Ang1) for 20 min. After fixation, the cells were immunostained with anti-α5 integrin antibody and visualised with Alexa 546-conjugated secondary antibody. Images of GFP (green) and Alexa 546 (red) are shown at the top and the second panels, respectively. Merged images of GFP and Alexa 546 and the phase-contrast images are shown on the third and the bottom panels, respectively. We used two kinds of siRNAs for α5 and β3. The results obtained from one siRNA for each target are shown (a, b, c, and d). **(e)** Images at the time point (30 min) of **Fig. 3c** are enlarged. The boxed regions are enlarged at the bottom. Note that Tie2-GFP clearly colocalises with Flag-tagged COMP-Ang1 at the bottom of the cells. The scale bar represents 20 μm (b-e). The scale bar in the enlarged image represents 5 μm (e). **(f)** To estimate non-specific binding of Flag-tagged proteins to ECM, binding of Flag-tagged bacterial alkaline phosphatase (BAP) protein to ECM was examined by immunofluorescence analysis as described in the legend of **Fig. 3d**.

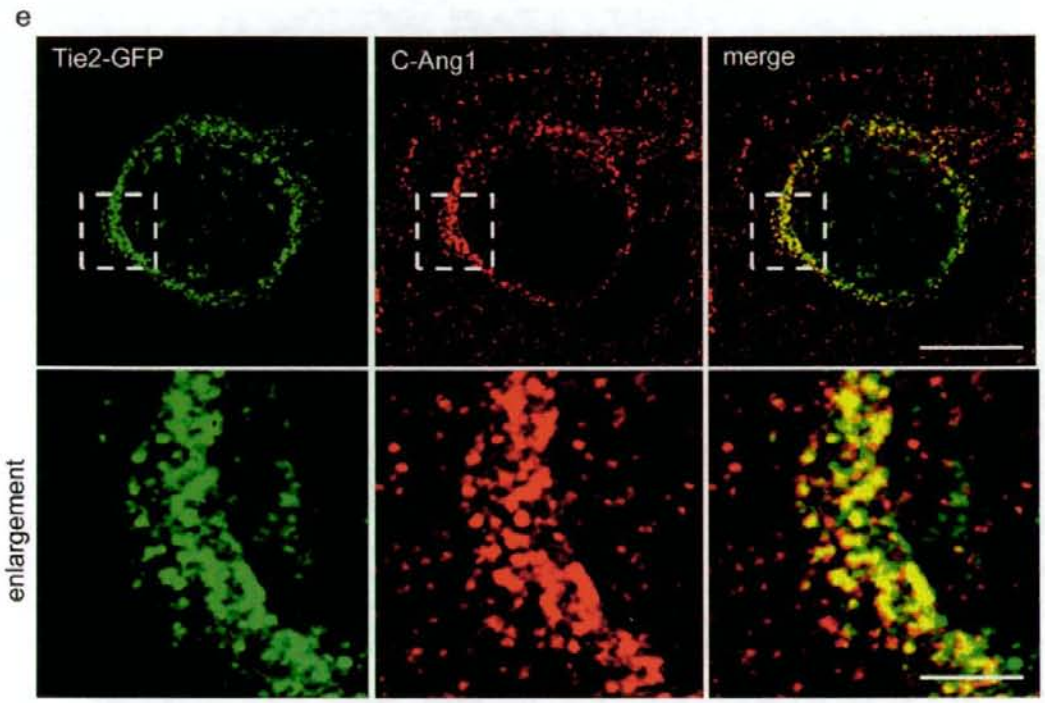

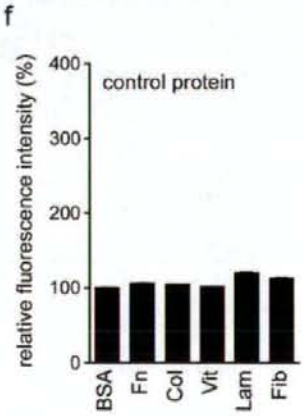

Figure S6 Continued

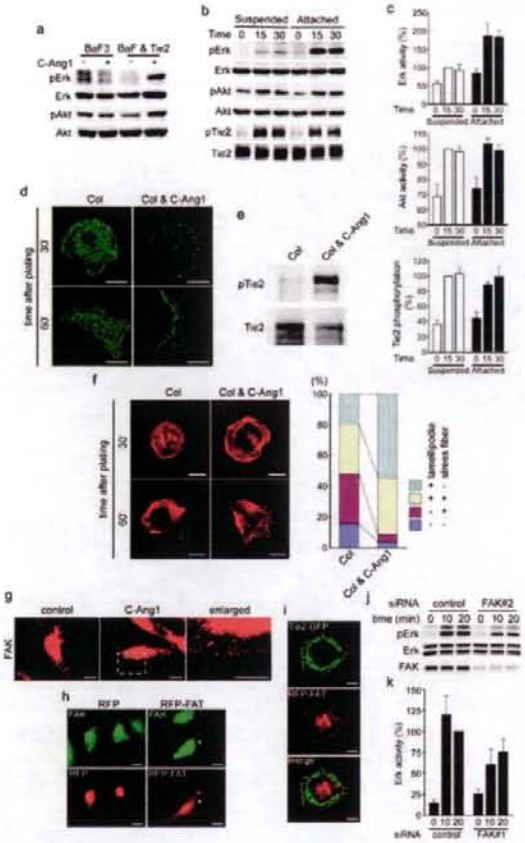

Figure S7 ECM-anchored Ang1 induces Tie2 signalling. **(a)** BaF3 and BaF-Tie2 cells placed on a fibronectin-coated dish were stimulated with vehicle (-) and COMP-Ang1 (+) for 15 min as described in Supplementary Methods. Erk and Akt activation was analyzed similarly to the legend of **Fig. 4d**. Phosphorylated and total Erk2, but not Erk1, were shown in the top and the second panels, since phosphorylated Erk1 was overlapped with non-specific bands. **(b)** Suspended BaF-Tie2 cells and the cells placed on a fibronectin-coated dish were stimulated with COMP-Ang1 for the time indicated on the top (min) as described in Supplementary Methods. Phosphorylation of Tie2, Erk, and Akt were analyzed as described in the legend of **Fig. 4b** and **4d,** respectively. **(c)** Phosphorylation of Erk, Akt and Tie2 observed in **b** was quantified as described in the legend of **Fig. 4c** and **4e,** and shown at top, middle, and bottom panels, respectively. Values are expressed as means ± standard deviations from five independent experiments. **(d)** COMP-Ang1 was bound to collagen-coated glass base dish as described in Supplementary Methods. HUVECs were placed on the COMP-Ang1-unbound collagen coated dish (Col) or COMP-Ang1-bound collagen-coated dish (Col & C-Ang1), for 30 (upper panels) and 60 min (bottom panels), and immunostained with anti-Tie2 antibody. Tie2 reacted with the primary antibody was visualized by Alexa 488-conjugated secondary antibody. Alexa 488 images of cell-substratum interface were obtained through a confocal microscope. **(e)** To examine whether ECM-bound COMP-Ang1 induces Tie2 signaling, starved HUVECs were placed on the COMP-Ang1-bound (Col & C-Ang1) or COMP-Ang1-unbound dish (Col) for 20 min as described in **d**. Cell lysates were immunoprecipitated with anti-Tie2 antibody. Immunoprecipitates and aliquots of cell lysate were subjected to Western blot analysis with anti-phosphotyrosine (pTie2) and anti-Tie2 (Tie2) antibodies, respectively. **(f)** HUVECs were stimulated as described in **d**, and stained with rhodamine-phalloidin. Rhodamine images were obtained through an epifluorescence microscope, and shown in left panel. The number of cells that produce lamellipodia and stress fibers identified by F-actin staining was counted. Accordingly, the cells were classified into four groups as follows; the cells that exhibit only lamellipodia, those that produce both lamellipodia and stress fibers, and those that exhibit only stress fibers, those that do not exhibit both lamellipodia and stress fibers (Col, n=102; Col & C-Ang1, n= 101). **(g)** Sparse HUVECs were stimulated with vehicle (left panel: control) or COMP-Ang1 (middle panel: C-Ang1) and immunostained with anti-FAK antibodies as described in the legend of **Fig. 3a**. FAK reacted with the primary antibody was visualized with Alexa 546-conjugated secondary antibody. The boxed area in the middle panel is enlarged (right panel). **(h)** HUVECs were transfected with either the vector encoding RFP or that encoding RFP-FAT, and stained with anti-FAK antibody. FAK reacted with the antibody was visualized with Alexa 488-conjugated secondary antibody. Alexa 488 and RFP images are shown in the upper and the lower panels, respectively. Asterisks indicate the cells expressing RFP-FAT. Note that FAK is replaced with RFP-FAT at the focal complexes and focal adhesions in the cell indicated by the asterisk. **(i)** Sparse HUVECs transfected with the plasmids encoding Tie2-GFP and RFP-FAT were starved for 3 h, and stimulated with COMP-Ang1 for 30 min. GFP, RFP and the merged images were shown at the top, the middle and the bottom panels, respectively. **(j)** HUVECs were transfected with control siRNA (control) or with FAK siRNA (FAK#2), which recognizes different sequence of FAK from that targeted by FAK#1 siRNA used in Fig. 5i. The cells were then starved and stimulated with COMP-Ang1 for the time (min) as indicated at the top similarly to the legend of **Fig. 4b**. Cell lysates were subjected to immunoblot analysis using anti-phospho-Erk (pErk) and anti-Erk (Erk) antibodies to assess Erk activity and with FAK antibody (FAK). **(k)** Erk phosphorylation induced by COMP-Ang1 stimulation observed in **j** was quantified as described in the legend of **Fig. 4e**. Values are expressed as means ± standard deviations from six independent experiments. The scale bars represent 20 μm (d, f, g, h, and i) and 5 μm (enlarged image in g), respectively.

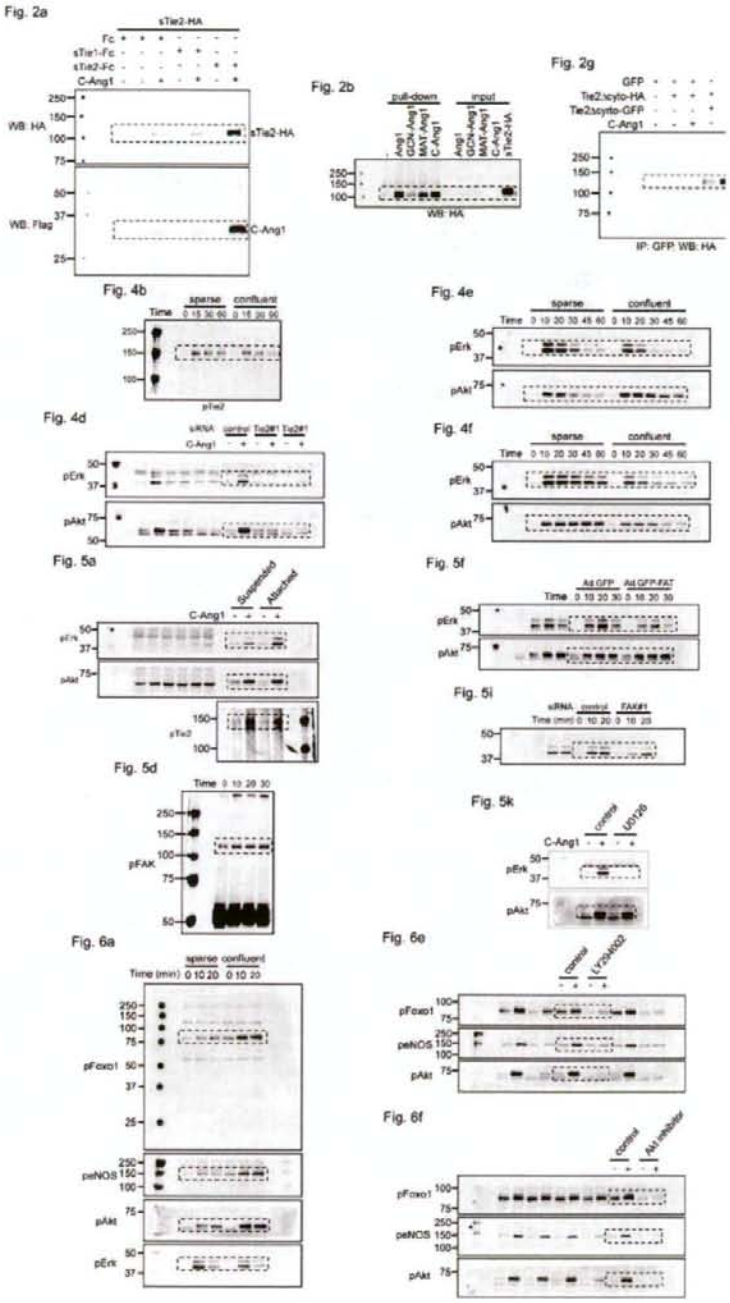

Figure S8 Full-scan images of key Western blots.